ACCELERATOR TECHNIQUES AND NUCLEAR ATA NEEDS FOR ION BEAM ANALYSIS OF WALL MATERIALS IN CONTROLLED FUSION DEVICES

M. RUBEL[1,2], D. PRIMETZHOFER[2], P. PETERSSON[1]
[1] KTH Royal Institute of Technology, Department of Plasma Physics Stockholm, Sweden
[2] Uppsala University, Department of Physics and Astronomy Uppsala, Sweden
Email: rubel@kth.se

S. CHARISOPOULOS [3]
[3] NAPC/Physics Section, International Atomic Energy Agency Vienna, Austria

Abstract

A brief overview of ion beam analysis methods and procedures in studies of materials exposed to fusion plasmas in controlled fusion devices with magnetic confinement is presented. The role of accelerator techniques in the examination and testing of materials for fusion applications is emphasised. Quantitative results are based on robust nuclear data sets, i.e. stopping powers and reaction cross-sections. Therefore, the work has three major strands: (i) assessment of fuel inventory and modification of wall materials by erosion and deposition processes; (ii) equipment development to perform cutting-edge research; (iii) determination of nuclear data for selected ion- target combinations. Underlying physics, advantages and limitations of methods are addressed. A note is also given on research facilities with capabilities of handling radioactive and beryllium-contaminated materials.

1. INTRODUCTION

Energy research driven by the quest for effective sources and means of electricity production is crucial for sustainable development. Despite distinct progress in energy-saving technologies and increasing number of installations based on fossil-free sources, the demand for electricity generation is ever growing to ensure functioning of transport, lighting, tele-communication and all branches of industry which require stable high-power supply. Simultaneously strong emphasis is on the safe and environmentally sound means of energy generation, while the production volume may be limited by the access to natural resources, currently available technologies, climate and, also by political situation.

Development of future technologies like Generation IV nuclear reactors and controlled thermonuclear fusion has a long history. In both cases, integrated efforts in science and technology are directed towards the construction and operation of reactor-class facilities. Controlled fusion is a multidisciplinary field encompassing plasma and ion physics, remote handling (RH) and radiofrequency (RF) technologies, nuclear physics and chemistry, demanding civil engineering, radiation protection and countless aspects of materials science and engineering: from the composition and structure of concrete for a base of a reactor containment to the detailed characterisation of the plasma-facing wall: plasma-facing materials (PFM) and components (PFC); both abbreviated jointly in the following as PFMC. The surface state of the latter class of materials is studied mainly by accelerator-based methods commonly called ion beam analysis (IBA).

In the interdisciplinary field of fusion research, the role of particle accelerators is at least five-fold: (i) ion beam analysis (IBA) of materials retrieved from vacuum vessels of controlled fusion devices; (iii) ion-induced simulation of neutron radiation effects in surfaces of solids; (iii) provision of nuclear data for ion-material interactions; (iv) ion-induced neutron generation for the material irradiation facility; (v) high current units in the neutral beam injection system for plasma (deuterium and tritium: D and T) heating. The first three aspects will be presented in the following sections with a focus on the role of accelerator techniques in the examination and testing of materials for fusion applications. Quantitative results can only be obtained using highly advanced laboratory equipment and combined with robust sets of nuclear data, i.e., stopping powers and reaction cross-sections. Therefore, the work has three essential strands: (a) assessment of fuel inventory and modification of PFMC composition by erosion and deposition processes; (b) equipment development to perform cutting-edge research; (c) determination of nuclear data for selected ion-target combinations.

2. CONTROLLED FUSION AND PLASMA-WALL INTERACTIONS: IMPACT ON MATERIALS

The goal of controlled thermonuclear fusion is to harness energy that powers stars: reactions of light nuclei characterised by Q values of several MeV and high reaction rates:

$$D + D \rightarrow T\ (1.01\ MeV) + H\ (3.03\ MeV) \quad (1a)$$

$$D + D \rightarrow {}^{3}He\ (0.82\ MeV) + n\ (2.45\ MeV) \quad (1b)$$

$$D + T \rightarrow {}^{4}He\ (3.52\ MeV) + n\ (14.06\ MeV) \quad (2)$$

$$D + {}^{3}He \rightarrow {}^{4}He\ (3.67\ MeV) + H\ (14.69\ MeV) \quad (3)$$

the branching ratio of Reactions 1a and 1b is around one. Deuterium fuel is used in most present-day devices, but the Q value (17.58 MeV) and the cross-section of the D-T process [1,2], favors that mix of hydrogen isotopes as a fuel for a reactor in a future power station. Reaction 3 has a significantly lower cross-section than Reaction 2 and, currently cannot be considered because of a very limited availability of ^{3}He.

Two major schemes of fusing nuclei have been developed. Inertial confinement fusion (ICF) uses high power photon (laser) [3] or ion beams [4] focused on a small (~1 mm in diameter) D-T containing pellet placed in a vacuum chamber of a few meters in diameter. Magnetic confinement fusion (MCF) based on plasmas generated and maintained by magnetic fields of a few T in toroidal systems [1,5]. The latter scheme exploits two reactor concepts: tokamaks [1,6] and stellarators [7]. In either case, both ICF and MCF, under terrestrial conditions the fusion plasma must be surrounded by walls of a vacuum vessel and, the energy released must then be absorbed by wall structures: 20% related to ^{4}He (α particles) by PFMC [8], while the neutron energy (80% of the total) is to be transferred to a ^{6}Li-enriched blanket where the conversion to heat and tritium production will occur [9,10]. The energy confinement time (τ_E) of particles of (up to 1.0-1.5 s) is shorter than the plasma discharge time.

Consequently, particles escape the plasma and impinge on the wall. These are electrons, ions at different ionisation states and charge exchange neutrals (CXN). In addition, there are neutrons generated in fusion reactions as well as electromagnetic radiation with a broad spectrum from RF down to hard gamma and X-rays. They are decisive for what is called plasma-wall interactions (PWI) which involve a huge range of processes: physical sputtering, chemical erosion, reflection, implantation, gas retention, desorption, melting, boiling, splashing, arcing, cracking, ionisation, recombination, compound formation, activation and consequential transmutation [8,11-13]. All of them are dynamic arising from atomic, molecular and nuclear physics and chemistry.

A scheme of interactions is shown in Figure 1. Eroded species are immediately ionised and travel along the magnetic field lines. Eventually, if not pumped out, the migrating species are re-deposited in a close or distant location with respect to the place of origin. Re-deposition involves atoms of different elements originally eroded from the wall. It is a simultaneous co-deposition in which also fuel atoms are included. As a result, mixed material layers are formed. The composition and other properties of such deposition zones significantly differ from those of the original substrates. Thermo-mechanical incompatibility between the substrate and co-deposit may lead to flaking and spalling-off of the layer thus forming dust which constitute a major operational issue if large amounts of dust are formed and, if such particles contain considerable fraction (a few atomic %) of fuel atoms, especially radioactive tritium or neutron- activation products.

In short, PWI comprises all processes of energy and mass exchange between the plasma and the surrounding surfaces. As a result, the plasma and the wall are modified with serious consequences for reactor operation. The plasma gets contaminated and loses energy, while properties of PFMC and some crucial tools for plasma diagnosis (mirrors and windows) are changed. This has an impact on the material lifetime and fuel inventory thus for the reactor safety. However, plasma-wall interactions are unavoidable but also necessary. The wall provides vacuum conditions indispensable for operation, removes heat and – only under D-T reactor conditions - ensures final thermalization of helium ash to enable its pump out and, absorption of energetic neutrons in the blanket for tritium productions and power generation.

In-vessel materials must be, in the first place, compatible with vacuum and strong magnetic fields, while the list of requirements for PFC candidates comprises in addition: high thermal conductivity (λ), i.e. over 150 m^{-1} K^{-1}, resilience to thermal shocks, low erosion yield by plasma species, low sorption of hydrogen isotopes to limit fuel inventory, high melting (T_m) and boiling (T_b) points, low-Z to minimise plasma energy losses by impurities, low erosion rate, low affinity to fuel and to oxygen impurities towards the formation of volatile products, affinity to oxygen impurities towards their gettering to form solid oxides, low neutron-induced

activation. None of the known substances has properties fulfilling such requirements especially that some of them are contradictory. Therefore, the material selection is based on the approach that properties should change as little as possible under plasma impact.

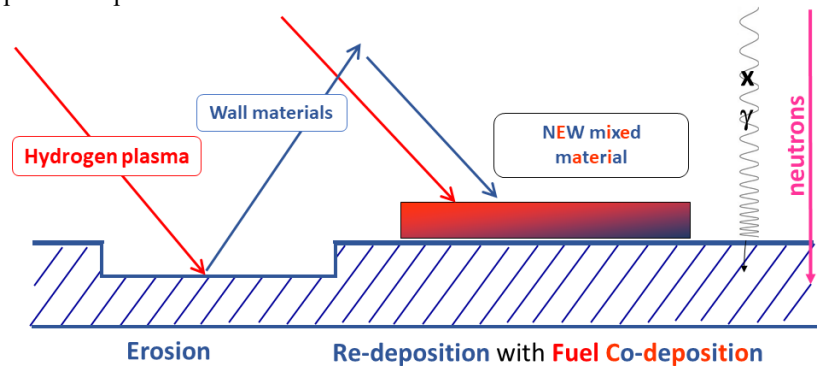

FIG. 1. Plasma-wall interactions: schematic illustration of erosion-deposition processes.

The major materials of interest for PFC are beryllium (Be), carbon (C) in the form graphite or carbon fibre composites (CFC), and tungsten (W). In addition, molybdenum (Mo) is important as material for so-called first mirrors, i.e., plasma-facing materials for optical diagnostics. Crucial advantages and drawbacks of respective wall materials are compiled in Table 1, while very detailed characteristic can be found in [8]. Graphite and several types of CFC have been used in toroidal devices since seventies of the 20th century because of their excellent power handling capabilities. Issues related to the erosion rates and the formation of fuel-rich co-deposits were known, but their dramatic seriousness was recognised after full D-T campaigns in TFTR [14,15] and JET [16-21] operated with carbon walls: nearly 30% of the injected tritium was retained in the vessel, especially in the remote areas of the divertor, i.e., places shadowed from the direct plasma line-of-sight. Such locations are very difficult to reach by any cleaning method [18,20,22]. No efficient means of fuel removal have been developed and the use of carbon in a D-T fusion reactor had to be reconsidered [22-27]. A large scale-test with all-metal walls was decided at the largest tokamak in the world: the Joint European Torus (JET) [28-30]. Carbon PFC were removed and replaced by solid Be limiters and Be coatings on the main chamber wall [31,32], while W components (bulk metal and coatings on CFC tiles) were installed in the divertor [32-34]. The operation of JET with the ITER-like wall (JET-ILW) started in 2011 and, it was clearly shown that the elimination of carbon sources resulted in a significant decrease of fuel retention [35-42] and dust generation [43-48]. In a consequence, the ITER Organisation decided to abandon carbon components in the divertor and prepare for operation with Be panels in the main chamber and tungsten in the divertor [49].

TABLE 1. Key properties of C and metals as wall materials and diagnostic components.

Element	Advantages	Drawbacks/Limitations	Remarks
C	Low-Z. Resilience to thermal shocks and no melting λ of some CFC > 300 W $m^{-1}K^{-1}$.	Chemical erosion by fuel atoms, C_xH_y formation, high erosion rate and fuel inventory in co-deposits.	PFMC in most tokamaks [8,14- 21,27,50-55] and stellarators [56-58] because of excellent power handling capabilities.
Be	Low-Z, no chemical erosion	Low T_m and high sputter yield.	Used in JET-ILW in the main chamber wall [29,31,59]; the same decided for ITER wall [49].
W	High T_m and low sputter yield by fuel	High-Z, risk for plasma contamination and disruptions. Activation and transmutation.	ASDEX Upgrade wall and divertor [60-61]. JET-ILW divertor [29,32-34,62]; the same decided for ITER divertor [49].
Mo	High T_m and low sputter yield by CXN	High activation.	Tested candidate for first mirrors in ITER diagnostic systems [63-67]

The major research objectives are to determine: (i) the lifetime of PFMC, (ii) in-vessel fuel accumulation, i.e., to obtain quantitative mapping of the distribution of D and T, (iii) quantity and properties of dust with particular emphasis on the identification of sources, generation pathways and fuel content, (iv) plasma impact on diagnostic components which are crucial for plasma characterisation and machine protection. All of them are decisive for reactor economy and safety. As such, these are key points in the licensing process. Conditio sine qua non for conclusive studies is the access to materials (specimens from diverse locations: wall tiles, probes, dust) retrieved from the vacuum vessel after experimental campaigns. Research requires a huge variety of material characterisation methods which directly implies the access to laboratories with relevant apparatus, competent research teams and – in many cases – capabilities and certificates for handling radioactive materials: T-contaminated and activated.

3. ANALYSIS METHODS AND INSTRUMENTATION

3.1 Challenges and Solutions **Analysis: Needs and Methods**

Over the years, more than fifty different material characterisation techniques have been used in the PFMC research: ion, electron, neutron and optical spectroscopies, methods based on probing solids with magnetic field, sound waves, mechanical force or thermal means applying either a steady temperature rise or shocks by flash heating. The variety of probing ('signal in') and detection means ('signal out'), their broad energy spectrum and a range of physical processes involved in the interactions create a huge number of "signal in – signal out" combinations, and – by this – research opportunities. Nearly every combination may actually be applied in a certain area of material characterization. However, only most efficient, methods for analyses of PFMC are mentioned in the following, i.e., techniques capable of sensitive and selective quantitative determination of the content and distribution (in-depth and lateral) of a wide range of elements and, in many cases, their particular isotopes present in the examined materials. Capabilities for mapping surface species on large areas on the tiles (e.g., 10x20 cm) are also required in many cases. Compositional analyses must cover a broad range of species which constitute wall and diagnostic components, fusion fuel and gases injected for auxiliary plasma heating, plasma edge cooling, disruption mitigation, wall conditioning or as markers (tracers) in material migration studies. As a result, the list extends from H, D, T, ^{3}He, ^{4}He and other noble gases (Ne – Xe), isotopes of Li, Be, B, C, N, O, F to heavier species such as Al, Si to Cr, Fe, Ni and then to W, Re, even Au is to be taken into account. The role and origin of respective species in the reactor is addressed in Table 2 in which also the information on relevant analysis methods is conveyed.

The requirement for lateral mapping and depth profiling of such diverse compositions are met by IBA methods. Their detailed description with physics basis can be found in [68,69], while the role in PFMC analysis has been addressed in overview articles [70-72]. IBA is based on the irradiation of a solid target with an ion beam and then detection and analysis of energy and/or mass spectra of signals emitted from the surface: reflected primary ions, products of nuclear reactions, recoiled atoms, photons (from visible to X and gamma rays), sputtered species such as secondary ions (monoatomic and molecular) and neutrals. Dependent on the ion (type, energy) – signal combination there is a number of methods governed by different underlying physical processes.

- Rutherford Backscattering Spectrometry (RBS) mainly with $^{4}He^{+}$ in the 1.5 – 3 MeV energy range.
- Non-Rutherford Enhanced Proton Scattering (EPS) with H^{+} in the 0.5 – 2.5 MeV range.
- Nuclear Reaction Analysis (NRA) – a huge variety of analytical capabilities using low-Z ion beams: mainly $^{3}He^{+}$ (0.6 – 6 MeV) and H^{+}, but also D^{+}, ^{12}C, ^{15}N and ^{16}O ions. Respective nuclear reactions are in Table 2.
- Particle Induced X-ray Emission (PIXE) and/or Gamma Emission (PIGE) using a primary 1.5 – 4 MeV beams of H^{+}, $^{3}He^{+}$, $^{4}He^{+}$.
- Time-of-Flight Elastic Recoil Detection Analysis (ToF-ERDA) with ^{4}He+ or the high ion version (ToF-HIERDA) using for instance multiply charged ion beams of C^{n+}, Si^{n+}, Br^{n+} or I^{n+} beams. Depth profiling down to 700 nm.
- Accelerator Mass Spectrometry (AMS) in trace analysis of T, ^{10}B, 14C.
- Medium Energy Ion Scattering (MEIS) using a 100 – 400 keV $^{4}He^{+}$ beam.
- Secondary Ion Mass Spectrometry (SIMS) with primary beams of Ar^{+}, Cs^{+} or O^{-} of a few keV. The method is sensitive but the quantification in complex mixed-material co-deposits is difficult.

TABLE 2. Species to be analysed/determined and their role in a reactor.

Species	Origin and role in a reactor	IBA Method	Reaction (of practical use)*	Remarks and references
H	Wall cleaning - conditioning gas	NRA, ERDA	$^{1}H(^{15}N,^{4}He)^{12}C$	H is always present in vacuum systems; information depth below 1 μm; strong detrapping by the ^{15}N beam.
D	Fuel	NRA, ERDA, EPS	$^{2}D(^{3}He,^{1}H)^{4}He$	NRA is the main technique in D analysis [70-80]. Depth profiling in C-H layers to over 30 μm at 6 MeV [73]
T	Fuel	NRA, ERDA, AMS	$^{3}T(^{12}C,^{4}He)^{11}B$ $^{3}T\ (^{12}C,\ ^{1}H)^{14}C$ $^{3}T\ (D,^{4}He)n$	Use of IBA is limited. Low sensitivity of ^{12}C-^{3}T reactions ^{12}C-^{3}T reactions tried on JET materials [81], while the ^{2}D -^{3}T was used on TFTR tiles [82]. AMS in trace analysis [83].
^{3}He	Minority gas for ICRF heating	ERDA		[84]
^{4}He	Ash of D-T reaction; Wall cleaning - conditioning gas	ERDA		[84]
^{6}Li, ^{7}Li	Li-beam diagnostic, wall coatings	NRA, ERDA, PIGE	$^{7}Li(^{1}H,n\gamma)^{8}Be$	
^{9}Be	Wall material	NRA, ERDA	$^{9}Be(^{3}He,^{1}H)^{11}B$ $^{9}Be(^{2}D,^{1}H)^{10}Be$ $^{9}Be(^{2}D,^{4}He)^{7}Li$	[20,71,72,75,77,85]
^{10}Be	Be migration marker	AMS		Marker n-activated ^{9}Be tile [86]
^{10}B and ^{11}B	Wall conditioning by low plasma in B_2H_6, $B(CH_3)_3$ or evaporation from $B_{10}H_{14}$	NRA, ERDA	$^{11}B(^{1}H,^{4}He)^{8}Be$ $^{11}B(^{3}He,^{1}H)^{13}C$	Analysis of PFMC from boronised machines [87-91]
^{12}C	Wall material	NRA, EPS, ERDA	$^{12}C(^{3}He,^{1}H)^{14}N$ $^{12}C(^{2}D,^{1}H)^{13}C$ $^{12}C(^{1}H,^{1}H)^{12}C$	[18,70-72,77,78,92] $^{12}C(^{2}D,^{1}H)^{13}C$ for C analysis on Be targets [85]
^{13}C	Tracer in C migration studies	NRA, EPS, ERDA	$^{13}C(^{3}He,^{1}H)^{15}N$ $^{13}C(^{1}H,^{1}H)^{13}C$	[93-96]
^{14}N	Edge cooling	NRA, ERDA	$^{14}N(^{2}D,^{1}H)^{15}N$ $^{14}N(^{2}D,^{4}He)^{12}C$	[85,93,97,98]
^{15}N	Tracer	NRA, ERDA	$^{15}N(^{1}H,^{4}He\ \gamma)^{12}C$	[96,98-100]
^{16}O	Major impurity	RBS, EPS, NRA, ERDA	$16O(^{2}D,^{1}H)^{17}O$ $^{16}O(^{1}H,^{1}H)^{16}O$	[93]
^{18}O	Tracer for in-vessel oxidation studies	NRA, ERDA	$^{18}O(^{1}H,^{4}He)^{15}N$	[65,78]

*Only reactions of practical use are listed, i.e. reactions with the detection limit of minimum $5x10^{14}$ cm^{-2}.

TABLE 2. (cont'd).

Species	Origin and role in a reactor	IBA Method	Reaction (of practical use)*	Remarks and references
^{20}Ne	Edge cooling agent	ERDA, RBS		[84,97]
^{21}Ne, ^{22}Ne	Considered as tracers	ERDA, RBS		RBS only on light substrates
Al	Impurity from structural material of RH systems	RBS, PIXE, ERDA		
Si	Component of in-vessel diagnostics	RBS, PIXE, ERDA		SiH_4 (SiD_4) used for wall conditioning (siliconisation) [101]
Ar	Edge cooling agent	RBS, PIXE, ERDA		[94]
Fe, Cr, Ni	Vacuum vessel and antennae materials: Steel, Inconel	RBS, PIXE, ERDA		Separation with RBS is difficult. ERDA and MEIS allow for separation of Cr and Ni
Cu	Impurity from NBI system	RBS, PIXE, ERDA		PIXE in presence of Fe, Cr, Ni
Kr	Edge cooling agent	RBS, PIXE, ERDA		[94]
Mo	Vacuum vessel and antennae materials: Steel, Inconel; First mirrors	RBS, PIXE, ERDA		
W	Wall material	RBS, PIXE, ERDA		
Re	Proposed addition to W	RBS, PIXE, ERDA		Only PIXE in the presence of W
Au	In-vessel diagnostics: bolometers, coated mirrors	RBS, PIXE, ERDA		

*Only reactions of practical use are listed, i.e. reactions with the detection limit of minimum $5x10^{14}$ cm^{-2}.

For most techniques, besides ERDA, the standard lateral resolution determined by beam diameter is in the range 0.6-1.2 mm. Detailed mapping of species with a resolution of 1-30 μm is carried out (if needed) with μ-RBS, μ-NRA, μ-EPS and μ-PIXE, i.e., using micro-beams formed in a quadrupole-equipped beamline. In ERDA or HIERDA which are based on the target irradiation at a shallow angle (usually 22.5o) the beam spot is elongated: 1x4 mm.

Taking into account a range of ion beams, beam spot size, broad energy spectrum, tens of nuclear reactions and data processing software, the "toolbox" offers a huge number of analytical options. It is also clear that there is no single technique to address all needs taking into account the differences in the information depth and sensitivity for detecting respective species because these parameters are decided by energy-dependent stopping powers in ion-target systems, and by cross-sections of individual processes.

The IBA methods are complementary to each other and, they are complementary to other techniques for characterisation of PFMC and fuel inventory. In the case of light isotopes, particularly in fuel retention studies, ^{3}He-based NRA plays a prominent role. It is the only method to determine quantitatively the areal distribution and depth profiles of deuterium down to tens of micrometres in light substrates [73]. Micro-NRA facilities deuterium

mapping in regions of highly not uniform content of that isotope [102,103] and even in single grains of dust [104,105]. NRA complements results of the gas balance assessment in fusion devices [50,79,106,107] and thermal desorption spectroscopy (TDS) data [108] to obtain an overview of the global fuel retention. Determination of the fuel content in PFMC is crucial to obtain reference targets in the development of in-situ techniques: laser-induced desorption (LIDS), breakdown (LIBS) or ablation (LIAS) spectroscopy techniques [109-114].

In the third column of Table 2 ERDA is listed in every set of useful/recommended techniques. ToF- HIERDA is an extremely powerful tool in the determination of low-Z isotopes on surfaces, especially when using a gas ionization chamber (GIC) detector [115], as it has been shown in studies of PFMC and wall probes from the TEXTOR [89,90], JET [77], COMPASS [91] tokamaks, and from laboratory experiments on mirror testing [116]. A great advantage is a simultaneous analysis of H, D, ^{3}He and ^{4}He [84]. High mass resolution facilitates conclusive results in material migration studies which involve the injection of tracer gases labelled with rare isotopes such as $^{13}CH_4$ [90], $^{15}N_2$ [90], $^{18}O_2$ [65,84] when it is essential to discriminate between the main and minor isotopes, e.g., ^{12}C eroded from PFMC and the injected ^{13}C tracer. The GIC detector opens possibilities for applying other tracers: $^{10}B_2H_6$, ^{21}Ne, ^{22}Ne. Figure 2 shows a spectrum of species detected with a 42 MeV $^{127}I^{8+}$ beam on the PFC surface retrieved from the TEXTOR tokamak after experiments with $^{13}CH_4$ and $^{15}N_2$ tracers.

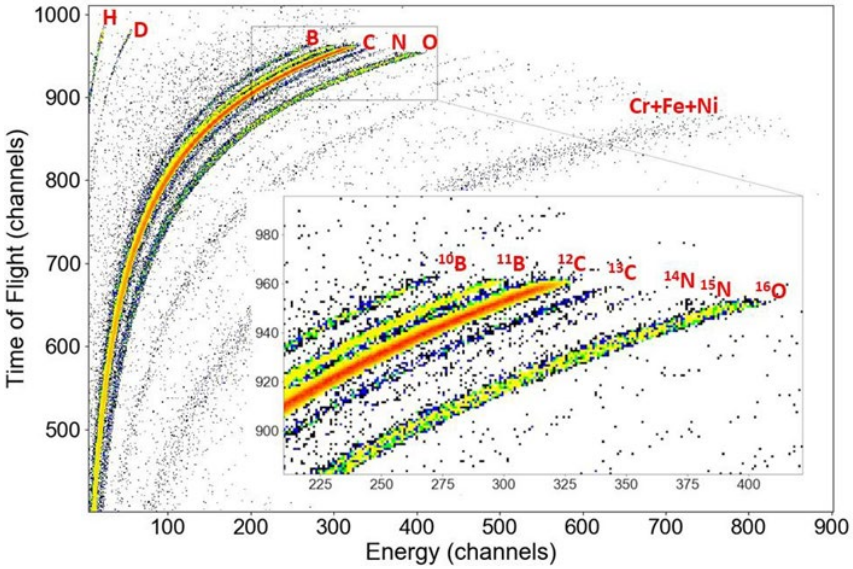

FIG. 2. ToF HIERDA spectrum recorded after tracer experiments for the limiter tile of TEXTOR.

3.2 Ion-induced damage in materials

The other role of accelerators in fusion research is in the ion-induced simulation of neutron damage in materials [10,116-118]. The damaged surface structure has a major impact on fuel retention in PFC and, also on optical performance of crucial diagnostic components like so-called first mirrors, i.e., metal mirrors acting as plasma-facing components in all optical plasma diagnosis systems (spectroscopy and imaging) in ITER, i.e., the reactor-class machine under construction. The impact of irradiation with H, ^{4}He (transmutation simulation) and Mo, Zr, Nb (simulation of n-induced damage) on the optically active layer of Mo mirrors has been presented [116-117]. There are three key points in such study: (i) the selection of irradiation conditions to by H, ^{4}He and high-Z species to influence changes in the optically active layer (OAL) of the mirror, i.e., maximum 30 nm of the outermost surface; (ii) the irradiation and determination of reflectivity changes; (iii) ToF HIERDA measurements of H and ^{4}He depth profiles, their changes in time and the dependence on the irradiation sequence. Plots in Figure 3(a) and (b) show, respectively, the depth profiles of H and He following the irradiation of polycrystalline Mo mirrors only with a 2 keV H^+ beam $14x10^{16}$ cm^{-2} and, first with $5x10^{16}$ cm^{-2} of 2 keV $^{4}He^+$ and then with $14x10^{16}$ cm^{-2} of 2 keV H^+. The results indicate that the damage produced by helium has a strong impact on the amount and depth distribution of hydrogen: the H profile is deeper when combined with He implantation. Secondly, the H retention is doubled after the He^+ irradiation in comparison to the irradiation with H^+ only: from 2% to 4% atomic.

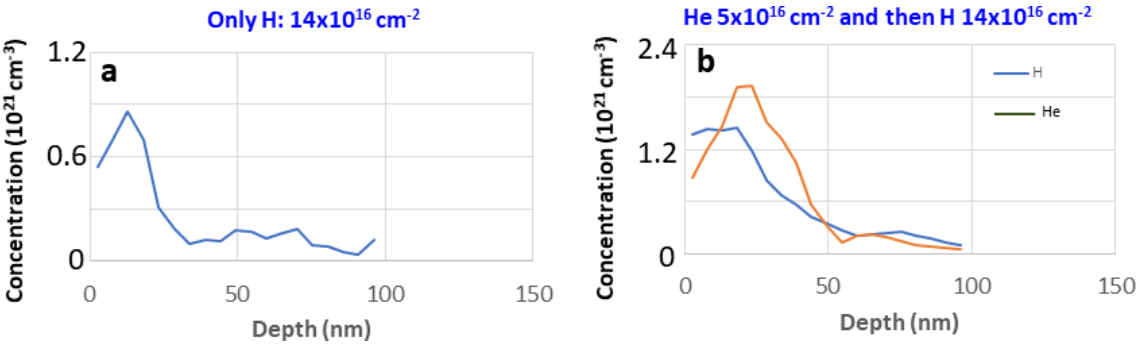

FIG. 3. ToF HIERDA depth profiles of H and He following two types of irradiation: (a) irradiation only with H; (b) irradiation with He followed by H.

3.3 Instrumentation

A pre-requisite for the advanced accelerator-based material research, either analysis or modification, is a laboratory (or a network of laboratories) with equipment providing a broad range of capabilities regarding the beam composition, energy, current, particle detection and, the control of experimental parameters: gas feed, temperature etc. A review of twelve accelerator laboratories with a detailed account on the facilities relevant to studies of fusion-related materials has been given in [72]. Among them, there are six laboratories capable of handling and analysing Be- and T- contaminated materials from JET: from full not sectioned Be tiles (12cm x 20cm) to smaller sectioned samples and dust. Work procedures with such materials (handling, transport etc.) have been addressed in [71,72], while very details are in [119].

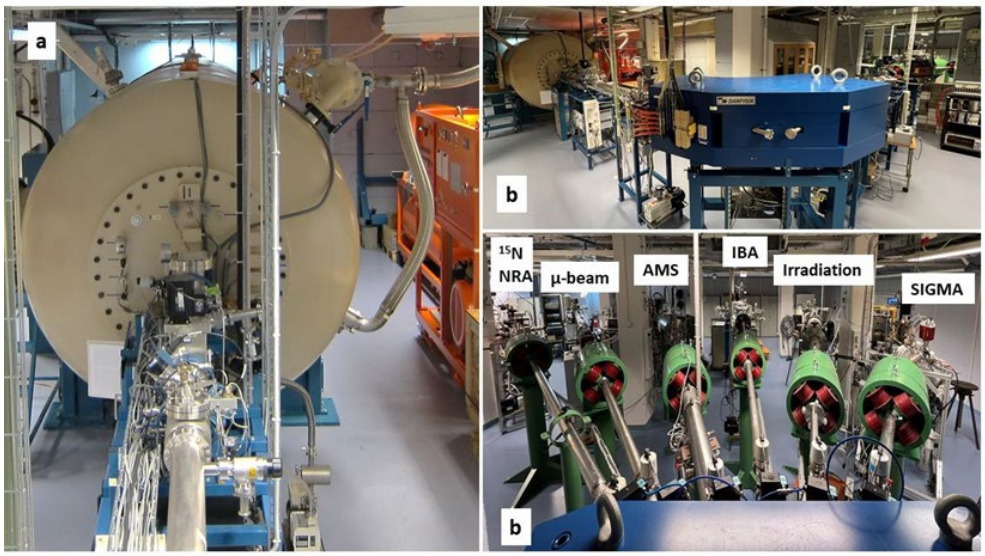

FIG. 4. Tandem Laboratory at the Uppsala University: (a) the accelerator; (b) analysing magnet; (c) six beamlines with the description of their main purpose.

New developments of the instrumentation are crucial to enhance and to broaden research capabilities. Images in Figure 4 show the 5 MV Pelletron Tandem (National Electrostatic Corporation, NEC) and the beamline arrangement at the Tandem Laboratory, Uppsala University, Sweden. Two gas and two sputter ion sources allow for the formation of beams in all mass ranges, from low-Z (H - Li), medium-Z (Be – Si) and, with some exceptions, high-Z up to Au. There are six beamlines for standard IBA (PIXE, RBS, NRA and ToF ERDA with GIC detector [115]) and very specific tasks like ^{15}N NRA with a gamma detector, AMS used mainly in the ^{10}Be [86] and ^{14}C analyses, μ-beam with PIXE, RBS, NRA. A separate line is dedicated to material modification by ion irradiation while the newly developed system on the sixth beamline is for in-situ and in-operando research: Set-up for *In- situ* Growth, Material modification and Analysis (SIGMA) [120,121].

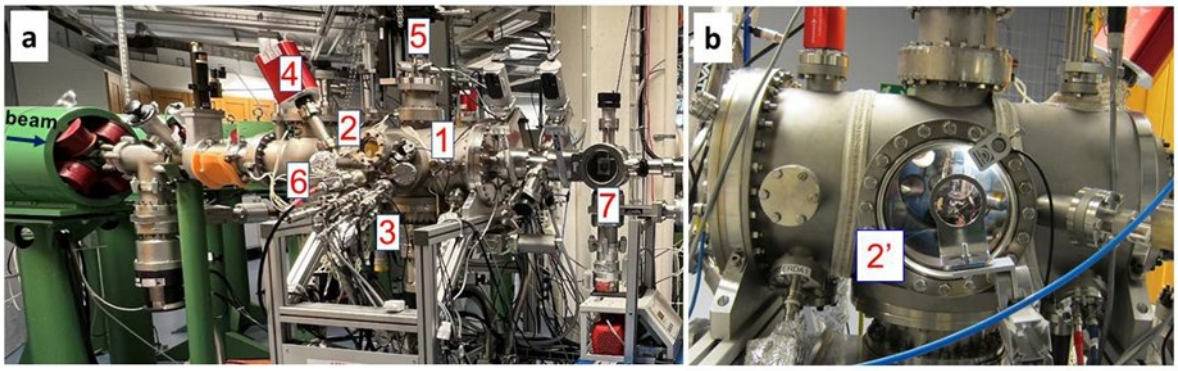

FIG. 5. SIGMA chamber – 1; viewing ports on both sides of the chamber – 2 and 2'; triple evaporator – 3; residual gas analyzer – 4; sample manipulator – 5; ion gun – 6; load-lock chamber – 7.

As already mentioned, all processes involved in PWI are dynamic. Direct in-situ material studies inside fusion devices are technically either very challenging or not possible at all. Some fundamental processes can therefore be investigated under controlled laboratory conditions. The SIGMA system, presented in Figure 5(a) and (b), has been designed to facilitate material modification with in-situ IBA employing both light and heavy beams for RBS, NRA, PIXE, PIGE, ToF-ERDA at the 2- 50 MeV energy range. Due to large viewing ports optical characterization is also carried out. Several gas feeds, three evaporation cells, a sputter gun (1-5 MeV) enable diverse material modification scenarios. Sample annealing to 1100 ºC combined with gas phase analysis offers a wide range of experimental possibilities in studies of fuel retention in fusion-relevant targets.

Two other accelerating systems at Uppsala University extend research on material modification [121]. With a 350 kV implanter (Danfysik) equipped with three changeable ion sources (gas, oven-based, sputter) the simulation of neutron-induced damage by means of light and heavy ion irradiation is carried on mirrors tested for diagnostic and heating systems in future fusion devices [116-118]. Two other beamlines are for: (i) ToF-MEIS and (ii) low energy RBS and NRA. The application of MEIS [77] ensured sensitive high-resolution determination of surface composition and has led to new topics in material migration.

A low energy ion gun (up to 10 kV) in another system equipped with two chambers is the base for ToF Low Energy Ion Scattering (ToF LEIS), Auger Electron Spectroscopy (AES) and Low Energy Electron Diffraction (LEED) [122]. Material modification capabilities annealing, sputtering and in-situ growth of thin layers. In all materials analyses, the quantification of composition is essential. In the case of IBA, it relies on the energy dependent cross-sections in the interactions of fast particles with matter.

4. STOPPING AND REACTION CROSS-SECTIONS

The energy deposition by energetic charged particles in matter is conveniently described by the energy deposition per unit path length, commonly referred to as stopping power (S). Dependent on the nature of the interaction, i.e. whether energy is deposited by elastic interaction between ion and target nuclei or by excitation of the electronic system of the target, one refers respectively to electronic (S_e) or nuclear (S_n) stopping power [123]. By a convenient transformation one obtains the stopping cross section by normalization by the atomic density N, which yields a quantity independent of the mass density of the target material. In any representation, accurate knowledge on the specific energy deposition of charged particles forms a key ingredient for quantification in ion beam analytical methods, by providing depth scales, in ion implantation by allowing for a prediction of particle range and in modelling of, e.g., sputtering processes and defect formation [69,124]. At high energies, the interaction with the target electronic system has been already early modelled successfully by Bethe [125] with subsequent further improvements [126-128]. Towards lower energies, interaction becomes more complex even for the lightest ions, as details of the electronic structure of the material were predicted to affect the energy deposition [129]. These effects of the density of states of the irradiated material were later been confirmed in several experiments for metals with excitation thresholds for specific electronic states [130-131] as well as for insulators featuring a band gap [132,133]. For light ions different from protons, also projectile excitation becomes increasingly relevant [134,135] still challenging predictions up to date [136-137]. In a similar fashion as

calculations feature an increasing complexity towards low ion energies, the same applies to experiments: stopping powers are experimentally most straightforwardly obtained in transmission experiments [138], for which, at lower energies, however the deteriorating influence of surface contaminations increases. In backscattering geometry, effects of surface contamination are drastically reduced, however, at lower energies, effects of plural and multiple scattering affect the spectra, complicating the analysis, requiring accurate simulations [139,140]. An additional option, available when sufficiently thin films of the target material cannot reliably be obtained is evaluation from the height of a spectrum recorded for a thicker film or bulk of the material of interest [141. In all cases, however, material purity is of utmost importance, which is challenging to guarantee for thin layers near a surface [142]. For all the reasons above, the database of electronic stopping powers hosted by IAEA [143,144] features only a limited number of datasets at low ion energies. Also, the materials, for which stopping powers have been measured or calculated is found limited [145]. The most commonly employed source for tabulated stopping powers, the semi empirical SRIM-code [146], is thus challenged in its predictive capacity. For many aspects of research on plasma-wall interaction is it, however, these low energies, which are most relevant. Low ion energies are not only relevant to model sputtering, fuel retention or defect formation, but are similarly necessary for quantification in analytical approaches such as Low- and Medium Energy Ion Scattering (LEIS & MEIS) [122,147]. Table 3, summarizes the status quo for a number of elemental target materials highly relevant for next generation fusion devices, indicating the almost complete absence of data at low energies, as well as the presence of an ambiguity of available data.

TABLE 3. Account on availability of the stopping powers data for selected elements.

Element	H ions	He ions
Be	No data below 10 keV – no reliable data below 1 MeV.	No data below 200 keV.
C	High number of datasets	High number of datasets; limitations at low energies.
Mo	No data below 50 keV – data spread in the stopping maximum.	Only one low-energy dataset – spread in the stopping maximum.
W	Only one dataset below 100 keV.	Only one dataset below 300 keV; two datasets differing by 10% at classical IBA energies.

Plots in Figures 6 and 7, show respectively detailed data for H in Be and He in W, thus illustrating the limited availability and reliability of reference data at intermediate energies or their complete absence at low energies respectively. Recently, the development of new computational approaches such as time-dependent density functional theory [148,149] or abandoning the modelling of a homogeneous electron gas [150] provides successively better predictions for specific systems, but commonly with high computational expenses. Dedicated experiments providing a better insight into the dependence of stopping powers on Z_2 [151] or specifically targeting materials for PFMC [152] enhance simultaneously the predictive power of semi-empirical approaches. Nevertheless, due to the large number of relevant ion-target combinations, energies and experimental approaches, a concerted action - as proposed by a number of research groups in the CRP-F11023 coordinated by IAEA - will be necessary to build up comprehensive knowledge for the relevant materials in the relevant energy range on the stopping of H and He in Be, Fe, Mo and W. A very similar lack of data and thus necessity for acquisition of high-quality reference data is found for reaction cross-sections of especially ^{3}He with isotopes of Li, Be, B, C, also N and O in the 1-6 MeV energy range.

5. CONCLUDING REMARKS

The accelerator-based analysis and modification of materials is not an isolated or a passive strand of fusion research. The results directly contribute to decisions regarding the wall composition and diagnostic planning in the current and future devices, e.g., ITER and DEMO. It is a driving force for improvements and development of analytical capabilities (nuclear data sets, detectors, chambers) to ensure cutting edge research. To keep this status, continual development of the methods in accordance with what was outlined above is required. Especially the role of in-situ and in-operando systems for the material modification and analyses will be crucial for a deep insight into the dynamics of fuel retention and segregation of metals in PFMC relevant materials such as EUROFER.

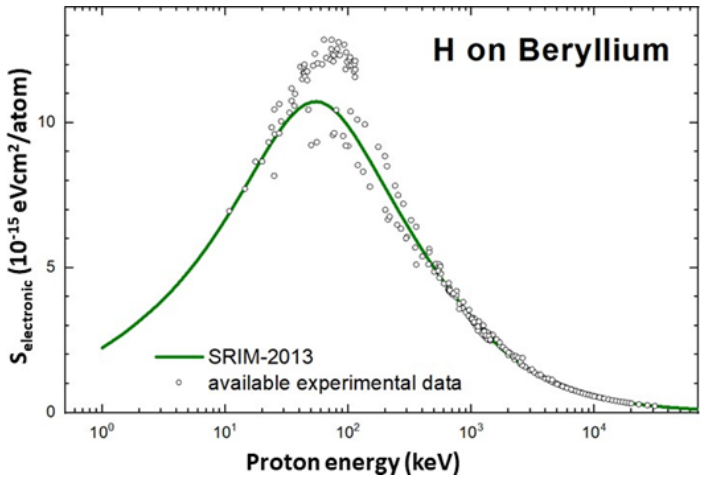

FIG. 6. Data availability of experimental reference electronic stopping cross-sections for hydrogen on beryllium.

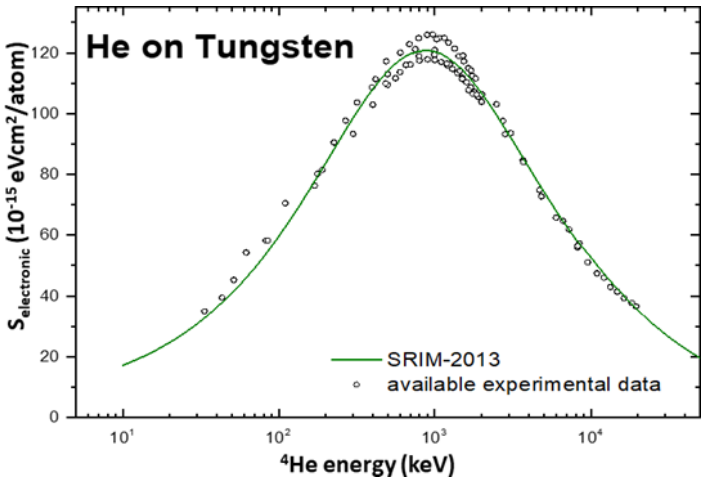

FIG. 7. Data availability on experimental reference electronic stopping cross-sections for helium-4 on tungsten.

ACKNOWLEDGEMENTS

The work has been supported by the Swedish Research Council (VR), Grant 2016–05380. Financial support of the Tandem Accelerator Infrastructure by VR-RFI (contract #2017–00646_9) as well as the Swedish Foundation for Strategic Research (SSF) under contract RIF14–0053 is gratefully acknowledged

REFERENCES

[1] WESSON J., Tokamaks, Oxford University Press, 3rd edition (2008).
[2] BOSCH H-S., HALLE G.M., Improved formulas for fusion cross-sections and thermal reactivities, Nucl. Fusion **32** (1992) 611-632.
[3] MOSES E., Advances in inertial confinement fusion at the National Ignition Facility (NIF), Fusion Eng. Des. **85** (2010) 983.
[4] HOFFMAN I., Review of accelerator driven heavy ion nuclear fusion, Matter Radiat. Extreme **3** (2018) 1.
[5] MIYAMOTO K., Plasma Physics for Controlled Fusion, Springer Series on Atomic, Optical, and Plasma Physics, vol. 92, Springer (2016).
[6] ARTSIMOVITSCH L.A., Tokamak devices, Nucl. Fusion **12** (1972) 215-251.

[7] SPITZER L., The stellarator concept, Phys. Fluids **1** (1958) 253-264.
[8] FEDERICI G. et al., Plasma-material interactions in current tokamaks and their implications for next step fusion reactors, Nucl. Fusion **41** (2001) 1967-2137.
[9] TANABE T. (Ed.), Tritium: Fuel of Fusion Reactors, Springer Verlag (2016).
[10] RUBEL M., Fusion Neutrons: Tritium breeding and impact on wall materials and components of diagnostic systems, J. Fusion Energy **38** (2019) 315-329.
[11] HOFER W.O., ROTH J. (Eds), Physical Processes of the Interaction of Fusion Plasmas with Solids, Academic Press, New York (1996).
[12] NAUJOKS D., Plasma-Material Interactions in Controlled Fusion, Springer Verlag (2006).
[13] PHILIPPS V., WIENHOLD P., KIRSCHNER A., RUBEL M., Erosion and redeposition of wall material in controlled fusion devices, Vacuum **67** (2002) 399-408.
[14] SKINNER C.H. et al., Plasma wall interaction and tritium retention in TFTR, J. Nucl. Mater. **241-243** (1977) 214-226.
[15] SKINNER C.H. et al., Tritium experience in large tokamaks: Application to ITER, Nucl. Fusion **39** (1999) 271-292.
[16] KEILHACKER M., WATKINS M.L., JET TEAM, D-T experiments in the JET tokamak, J. Nucl. Mater. **266-269** (1999) 1-13.
[17] ANDREW P. et al., Tritium retention and clean-up in JET, Fusion Eng. Design **47** (1999) 233-245.
[18] COAD J.P. et al., Erosion/deposition issues at JET, J. Nucl. Mater. **290-293** (2001) 224-230.
[19] PENZHORN R-D. et al., Tritium depth profiles in graphite and carbon fibre composite material exposed to tokamak plasmas, J. Nucl. Mater. **288** (2001) 170-178.
[20] RUBEL M. et al., Beryllium and carbon films in JET following D-T operation, J. Nucl. Mater. **313-316** (2003) 321-326.
[21] COAD J.P. et al., Material migration and fuel retention studies during the JET carbon divertor campaigns, Fusion Eng. Des. **138** (2018) 78-108.
[22] COUNSELL G.C., Tritium retention in next step devices and the requirements for mitigation and removal techniques, Plasma Phys. Control. Fusion **48** (2006) B189-B199.
[23] RUBEL M. et al., Fuel removal from plasma-facing components by oxidation-assisted technique. An overview of surface morphology after oxidation, J. Nucl. Mater. **363-365** (2007) 877-881.
[24] RUBEL M. at al., Fuel removal from plasma-facing components by oxidation techniques. An overview of surface
[25] HOPF C. et al., Oxygen glow discharge cleaning in ASDEX Upgrade, J. Nucl. Mater. **363-365** (2007) 882-887.
[26] ROTH J. et al., Tritium inventory in ITER plasma-facing materials and tritium removal procedures, Plasma Phys. Control. Fusion **50** (2008) 103001.
[27] RUBEL M. et al., Efficiency of Fuel Removal Techniques Tested on Plasma-Facing Components from the TEXTOR Tokamak, Fusion Eng. Des. **87** (2012) 935-940.
[28] MATTHEWS G.F. et al., ITER-Like Wall project overview, Phys. Scr. **T128** (2007) 137-143.
[29] MATTHEWS G.F. et al., Current status of the JET ITER-like Wall Project, Phys. Scr. **T138** (2010) 014030.
[30] MATTHEWS G.F. et al., Overview of the ITER-like wall project, Phys. Scr. **T145** (2011) 014001.
[31] RUBEL M. et al., Beryllium plasma-facing components for the ITER-Like Wall Project at JET, J. Phys. Conf. Series **100** (2008) 062028.
[32] MAIER H. et al., Tungsten and beryllium armour development for the JET ITER-like wall Project, Nucl. Fusion **47** (2007) 222-227.
[33] MERTENS Ph. et al., Clamping of solid tungsten components for the bulk W divertor row in JET—precautionary design for a brittle material, Phys. Scr. **T138** (2009) 014032.
[34] MERTENS Ph. et al., Detailed design of a solid tungsten divertor row for JET in relation to the physics goals, Phys. Scr. **T145** (2011) 014002.
[35] MATTHEWS G.F., Plasma operation with an all metal first-wall: Comparison of an ITER-like wall with a carbon wall in JET, J. Nucl. Mater. **438** (2013) S2-S10.
[36] LOARER T. et al., Comparison of fuel retention in JET between carbon and the ITER-Like Wall, J. Nucl. Mater. **438** (2013) S108-S113.

[37] WIDDOWSON A. et al., Overview of fuel inventory in JET with the ITER-like wall, Nucl. Fusion **57** (2017) 086045.
[38] WIDDOWSON A. et al., Overview of the JET ITER-like wall divertor, Nucl. Mater. Energy **12** (2017) 499-505.
[39] WIDDOWSON A. et al., Fuel inventory and material migration of JET main chamber plasma facing components compared over three operational periods, Phys. Scr. **T171** (2020) 014051. https://doi.org/10.1088/1402-4896/ab5350
[40] MAYER M. et al., Erosion and deposition in the JET divertor during the first ILW campaign, Phys. Scr. **T167** (2016) 014051.
[41] KRAT S. et al., Comparison of erosion and deposition in JET divertor during the first three ITER-like wall campaigns, Phys. Scr. **2020**, T171, 014059.
[42] BARON-WIECHEC A. et al., Global erosion and deposition patterns in JET with the ITER-like wall, J. Nucl. Mater. **463** (2015) 157-161.
[43] WIDDOWSON A. et al., Material migration patterns and overview of first surface analysis of the JET ITER-Like Wall, Phys. Scr. **T159** (2014)014010.
[44] BARON-WIECHEC A. et al., First dust study in JET with the ITER-Like Wall: Sampling, analysis and classification, Nucl. Fusion **55** (2015) 113033.
[45] FORTUNA-ZALESNA E. et al., Dust survey following the final shutdown of TEXTOR: Metal particles and fuel retention, Phys. Scr. **T167** (2016) 014059.
[46] FORTUNA-ZALESNA E. et al., Studies of dust from JET with the ITER-Like Wall: Composition and internal structure, Nucl. Mater. Energy **12** (2017) 582-587.
[47] LITAUDON X. et al**.,** Overview of the JET in support of ITER**,** Nucl. Fusion **57** (2017) 102001.
[48] RUBEL M. et al., Dust generation in tokamaks: Overview of beryllium and tungsten dust characterisation in JET with the ITER-like wall, Fusion Eng. Des. **136** (2018) 579-586.
[49] MEROLA M., et al., Overview and status of ITER internal components, Fusion Eng. Des. **89** (2014) 890-895.
[50] TSITRONE E. et al., Multi machine scaling of fuel retention in 4 carbon dominated tokamaks, J. Nucl. Mater. **415** (2011) S735-S739.
[51] WAMPLER W.R. et al., Erosion and deposition of metals and carbon in the DIII-D divertor, J. Nucl. Mater. **266-269** (1999) 791-797.
[52] ALLEN S.L. et al., ^{13}C transport studies in L-mode divertor plasmas on DIII-D, J. Nucl. Mater. **337-339** (2005) 30-34.
[53] LOARER T. et al., Gas balance and fuel retention in fusion devices, Nucl. Fusion **47** (2007) 1112-1120.
[54] MASAKI K. et al., Tritium distribution in the JT-60 W-shaped divertor, J. Nucl. Mater. **313-316** (2003) 514-518.
[55] KAMADA Y. et al., Completion of JT-60SA construction and contribution to ITER, Nucl. Fusion **62** (2022) 042002.
[56] TOKITANI M. et al., Microstructural characterization of mixed-material deposition layer on the LHD divertor tiles by using nano-geological diagnosis, J. Nucl. Mater. **438** (2013) S818-821.
[57] MAYER M. et al., Material erosion and deposition on the divertor of W7-X, Phys. Scr. **T171** (2020) 014035.
[58] BREZINSEK S. et al., Plasma-Surface Interaction in the Stellarator W7-X: Conclusion Drawn from Operation with Graphite Plasma-Facing Components, Nucl. Fusion **62** (2022) 016006.
[59] BREZINSEK S. et al., Beryllium migration in JET ITER-like wall Plasmas, Nucl. Fusion **55** (2015) 063021.
[60] NEU R. et al., Overview on plasma operation with a full tungsten wall in ASDEX Upgrade, J. Nucl. Mater. **438** (2013) S34-S41.
[61] NEU R. et al., Impurity behaviour in the ASDEX Upgrade divertor tokamak with large area tungsten walls, Plasma Phys. Control. Fusion 41 (2002) 811-826.
[62] BREZINSEK S. et al, Erosion, screening and migration of tungsten in the JET divertor, Nucl. Fusion **59** (2019) 096035.

[63] RUBEL M., Mirror Test for ITER at the JET tokamak: An overview of the programme, Rev. Sci. Instrum. **77** (2006) 063501-1 – 063501-6.
[64] IVANOVA D. et al., An overview of the Comprehensive First Mirrors Test in JET with ITER-Like Wall, Phys. Scr. **T159** (2014) 014011.
[65] MOON SUNWOO et al., First mirror test in JET for ITER: Complete overview after three ILW campaigns, Nucl. Mater. Energy **19** (2019) 59-66.
[66] LITNOVSKY A. et al., Diagnostic mirrors for ITER: research in a frame of International Tokamak Physics Activity, Nucl. Fusion **59** (2019) 066029.
[67] RUBEL M. et al., First mirror erosion-deposition studies in JET using an ITER-like mirror test assembly, Nucl. Fusion **61** (2021) 046022.
[68] CHU W.K., MAYER M., NICOLET M.A., Backscattering Spectroscopy, Academic Press, New York (1978).
[69] TESMER J.R., NASTASI M. (Eds), Handbook of Modern Ion Beam Analysis, Material Research Society, Pittsburg, PA (1995).
[70] RUBEL M, Analysis of plasma facing materials: material migration and fuel retention, Phys. Scr. **T123** (2006) 54-65.
[71] RUBEL M. et al., The role and application of ion beam analysis for studies of plasma-facing components in controlled fusion devices, Nucl. Instr. Meth. **B371** (2016) 4-11.
[72] MAYER M. et al., Ion beam analysis of fusion plasma-facing materials and components: facilities and research challenges, Nucl. Fusion **60** (2020) 025001.
[73] MAYER M. et al., Quantitative depth profiling of deuterium up to very large depths, Nucl. Instr. Meth. **B267** (2009) 506- 512.
[74] RUBEL M. et al., Fuel inventory and deposition in castellated structures in JET-ILW, Nucl. Fusion **57** (2017) 066027.
[75] DITTRICH L. et al., Fuel retention and erosion-deposition on inner wall cladding tiles in JET-ILW, Phys. Scr. **96** (2021) 124071.
[76] WIDDOWSON A. et al., Evaluation of tritium retention in plasma facing components during JET tritium operations, Phys. Scr. **96** (2021) 124075.
[77] STRÖM P. et al., Analysis of co-deposited layers with deuterium and impurity elements on samples from the divertor of JET with ITER-like wall, J. Nucl. Mater. **516** (2019) 202-213.
[78] GARCIA-CARRASCO A. et al., Impact of ion cyclotron wall conditioning on plasma-facing components, Phys. Scr. **T159** (2014) 014017.
[79] PÉGOURIÉ B. et al., Deuterium inventory in Tore Supra: coupled carbon – deuterium balance, J. Nucl. Mater. **438** (2013) S120-S126.
[80] RUBEL M., BREZINSEK S., WIDDOWSON A., "Surface modification by fusion plasmas", Plasma Applications for Material Modification: From Microelectronics to Biological Materials, Jenny Stanford Publishing, Singapore (2020).
[81] BYKOV I. et al., Investigation of tritium analysis methods for ion microbeam application, Nucl. Instrum. Meth. **B 273** (2012) 250-253.
[82] KUBOTA N. et al., "Surface Analysis for TFTR armour tile exposed to D-T plasmas using nuclear technique", 21st IAEA Conf. on Fusion Energy, EX/P4-12 (2006).
[83] FRIEDRICH M. et al., Tritium depth profiling by AMS in carbon samples from fusion experiments, Phys. Scr. **T94** (2001) 98-101.
[84] DITTRICH L. et al., "Retention of seeded gases in first wall components from the JET tokamak with the ITER-like wall", 32nd Symposium on Fusion Technology (Dubrovnik, Croatia, 2022).
[85] LAGOYANNIS A. et al., Surface Analysis of the ITER-like wall divertor Tiles at JET tokamak, Nucl. Fusion **57** (2017) 076027.
[86] BYKOV I. et al., Studies of Be migration in the JET tokamak using AMS with ^{10}Be marker, Nucl. Mater. **371** (2016) 370-375.
[87] GUDOWSKA I. et al., Fluxes of boron in the scrape-off plasma of TEXTOR following boronization, J. Nucl. Mater. **176- 177** (1990) 363-369.
[88] HAKOLA A. et al., Global transport of light elements boron and carbon in the full-W ASDEX Upgrade, J. Nucl. Mater. **415** (2011) S227-S230.

[89] STRÖM P. et al., Characterisation of layers formed on plasma-facing components in controlled fusion devices: role of heavy ion elastic recoil detection, Vacuum **122** (2015) 260-267.
[90] WECKMANN A. et al., Review of global migration, fuel retention and modelling after TEXTOR decommission, Nucl. Mater. Energy **17** (2018) 83-112.
[91] WECKMANN A. et al., Deuterium deposition patterns for fuel retention in the divertor of the COMPASS tokamak, Fusion Eng. Des. **179** (2022) 113118.
[92] COAD J.P., RUBEL M., WU C.H., The amount and distribution of deuterium retained in the JET divertor after the C and Be phases in 1994-5, J. Nucl. Mater. **241-243** (1997) 408-413.
[93] RUBEL M. et al., Accelerator-based ion beam analysis of fusion reactor materials, Vacuum **78** (2005) 255-261.
[94] RUBEL M. et al., Overview of tracer techniques in studies of material erosion, re-deposition and fuel inventory in tokamaks, J. Nucl. Mater. **329-333** (2004) 795-799.
[95] COAD J.P. et al., Overview of material re-deposition and Fuel retention studies at JET with the Gas Box divertor, Nucl. Fusion **46** (2006) 350-366.
[96] PETERSSON P. et al., Nuclear reaction and heavy ion ERD analysis of wall materials from controlled fusion devices: deuterium and nitrogen 15 studies, Nucl. Instr. Meth. **B 273** (2012) 212.
[97] RUBEL M., Nitrogen and Neon Retention in Plasma-Facing Materials, J. Nucl. Mater. **415** (2011) S223-S226.
[98] PETERSSON P. et al., Transport and retention studies in tokamaks using ^{15}N tracer gas, Phys. Scr. **T159** (2014) 014042.
[99] PETERSSON P. et al., Nuclear reaction and heavy ion ERD analysis of wall materials from controlled fusion devices: deuterium and nitrogen 15 studies, Nucl. Instr. Meth. **B 273** (2012) 212.
[100] PETERSSON P. et al., Injection of nitrogen-15 tracer into ASDEX Upgrade: New technique in material migration studies, J. Nucl. Mater. **438** (2013) S616-S619.
[101] RUBEL M. et al., Silicon fluxes in the scrape-off layer plasma during silicon-assisted operation of TEXTOR, J. Nucl. Mater. 220 - 222 (1995) 536 – 540.
[102] PETERSSON P. et al., Micro distribution of fuel and metal in carbon based plasma-facing components, Phys. Scr. **T145** (2011) 014014.
[103] RUBEL M. et al., Fuel inventory and deposition in castellated structures in JET-ILW, Nucl. Fusion **57** (2017) 066027.
[104] FAZINIĆ S. et al., Ion micro-beam analysis of dust particles and co-deposits from JET with ITER-like wallAnal. Chem. **90** (2018) 5744-5744.
[105] FAZINIĆ S. et al., Micro-analyses of dust particles generated in the JET tokamak with the ITER-Like Wall, Nucl. Fusion **60** (2020) 12606.
[106] MAYER M. et al., Hydrogen inventories in nuclear fusion devices, J. Nucl. Mater. **290-293** (2001) 381-388.
[107] LOARER T. et al., Gas balance and fuel retention in fusion devices, Nucl. Fusion **47** (2007) 1112.
[108] HEINOLA K. et al., Long-term fuel retention in JET ITER-like wall, Phys. Scr. **T167** (2016) 014075.
[109] SUMMERS D.D.D. et al., In-situ measurement of hydrogen retention in JET carbon tiles, J. Nucl. Mater **290-293** (2001) 496-500.
[110] HUBER A. et al., In-situ measurement of trapped hydrogen by laser desorption in TEXTOR-94, Phys. Scr. **T94** (2001) 102-105.
[111] SCHWEER B. et al., In-situ diagnostic for monitoring of deuterium and tritium in re-deposited carbon layers by laser induced desorption, J. Nucl. Mater **363-365** (2007) 1375-1379.
[112] PHILIPPS V. et al., Development of laser-based techniques for in-situ characterization of the first wall in ITER and future fusion devices, Nucl. Fusion **53** (2013) 093002.
[113] MALAQUIAS M. et al., Development of ITER relevant laser techniques for deposited layer characterization and tritium inventory, J. Nucl. Mater. **438** (2013) S936-S939.
[114] ZLOBINSKI M et al., Efficiency of layer-induced desorption of D from Be/D layers and surface modification due to LID, Phys. Scr. **T171** (2020) 014075.
[115] STRÖM P. et al., A combined segmented anode gas ionization chamber and time-of-flight detector for heavy ion elastic recoil detection analysis, Rev. Sci. Instrum. **87** (2016) 103303.

[116] GARCIA-CARRASCO A. et al., of helium implantation and ion-induced damage on reflectivity of molybdenum mirrors, Nucl. Instr. Meth. **B 382** (2016) 91-95.
[117] RUBEL M. et al., Metallic mirrors for plasma diagnosis in current and future reactors: Tests for ITER and DEMO, Phys. Scr. **T170** (2017) 014061.
[118] SCHWARZ-SELINGER T., Deuterium retention in MeV self-implanted tungsten: Influence of damaging dose rate, Nucl. Mater. Energy **12** (2017) 683-688.
[119] WIDDOWSON A. et al., Experience of handling beryllium, tritium and activated components from JET ITER like wall, Phys. Scr. **T167** (2016) 014057.
[120] KANTRE K. et al., Combination of in-situ ion beam analysis and thermal desorption spectroscopy for studying deuterium implanted in tungsten, Phys. Scr. **96** (2021) 124004.
[121] STRÖM P., PRIMETZHOFER D., Ion beam tools for nondestructive in-situ and in-operando composition analysis and modification of materials at the Tandem Laboratory in Uppsala, J. Intrum. (JINST) **17** (2022) P04011.
[122] J. SHAMS-LATIFI J. et al., An *in-situ* ToF-LEIS and AES study of near-surface modifications of the composition of EUROFER97 induced by thermal annealing, Nucl. Mater. Energy **30** (2022) 101139.
[123] SIGMUND P., *Particle Penetration and Radiation Effects*, Vol. 2, Springer, Switzerland (2014).
[124] SAND A.E., NORDLUND K., J. Nucl. Mater. 456 (2015) 99-105.
[125] H. BETHE H., Zur Theorie des Durchgangs schneller Korpuskularstrahlen durch Materie, Ann. Physik 5 (1930) 325- 400.
[126] BETHE H., Bremsformel für Elektronen relativistischer Geschwindigkeit., Z. Physik 76 (1932) 293–299.
[127] MÖLLER C, Zur Theorie des Durchgangs schneller Elektronen durch Materie, Ann. Physik 406 (1932) 531-585.
[128] BLOCH F., Zur Bremsung rasch bewegter Teilchen beim Durchgang durch Materie, Ann. Physik 408 (1933) 285-320 and; Bremsvermögen von Atomen mit mehreren Elektronen, Z. Physik 81 (1933) 363-376.
[129] FERMI E., TELLER E., The Capture of Negative Mesotrons in Matter, Phys. Rev. 72 (1947) 399-408.
[130] VALDES J.E. et al, Energy loss of slow protons in solids: Deviation from the proportionality with projectile velocity, Phys. Rev. A 49 (1994) 1083-1088-2695.
[131] MARKIN S.N. et al., Electronic stopping of low-energy H and He in Cu and Au investigated by time-of-flight low- energy ion scattering, Phys. Rev. B 80 (2009) 205105.
[132] AUTH C. et al, Threshold in the Stopping of Slow Protons Scattered from the Surface of a Wide-Band-Gap Insulator, Phys. Rev. Lett. **81** (1999) 4831-4834.
[133] MARKIN S.N., PRIMETZHOFER D, BAUER P., Vanishing Electronic Energy Loss of Very Slow Light Ions in Insulators with Large Band Gaps, Phys. Rev. Lett. **103** (2009) 113201.
[134] PRIMETZHOFER D. et al., Electronic Excitations of Slow Ions in a Free Electron Gas Metal: Evidence for Charge Exchange Effects, Phys. Rev. Lett. **107** (2011) 163201.
[135] LOHMANN S., PRIMETZHOFER D., Disparate Energy Scaling of Trajectory-Dependent Electronic Excitations for Slow Protons and He Ions, Phys. Rev. Letters **124** (2020) 096601.
[136] LI, C-K, et al, *Ab initio* electronic stopping power and threshold effect of channelled slow light ions in HfO_2, Phys. Rev. **B 96** (2017) 094301.
[137] QUASHIE E.E, A.A. CORREA A.A., Electronic stopping power of protons and alpha particles in nickel, Phys. Rev. **B 98** (2018) 235122.
[138] MERTENS P., How to measure absolute stopping cross sections by backscattering and transmission methods: Part II. Transmission, Nucl. Instr. Meth. **B 27** (1987) 315-322.
[139] BAUER P., SEMRAD D., MERTENS P., Reference proton stopping cross sections for five elements around the maximum, Nucl. Instr. Methods Phys. Res., Sect. **B12** (1985) 56–61.
[140] BIERSACK J.P., STEINBAUER E., BAUER P., A particularly fast TRIM version for ion backscattering and high energy ion implantation, Nucl. Instr. Meth. **B 61** (1991) 77–82.
[141] ROTH D. et al., A procedure to determine electronic energy loss from relative measurements with TOF-LEIS, Nucl. Instr. Meth. **B 317** (2013) 61-65.

[142] ROTH D. et al., Systematic analysis of different experimental approaches to measure electronic stopping of very slow hydrogen ions, Nucl. Instr. Meth. **B 437** (2018) 1–7.
[143] Stopping Power Database. Available at: https://www-nds.iaea.org/stopping/
[144] MONTANARI C.C., DIMITRIOU P., The IAEA stopping power database, following the trends in stopping power of ions in matter, Nucl. Instr. Meth. **B 408** (2017) 50-55.
[145] WITTMAACK K., Misconceptions impairing the validity of the stopping power tables in the SRIM library and suggestions for doing better in the future, Nucl. Instr. Meth. **B 380** (2016) 57-70.
[146] ZIEGLER J.F, ZIEGLER M.D., BIERSACK J.P., SRIM – The stopping and range of ions in matter (2010), Nucl. Instr. Meth. **B 268** (2010) 1818-1823.
[147] KOSLOWSKI H.R. et al., Temperature-dependent in-situ LEIS measurement of W surface enrichment by 250 eV D sputtering of EUROFER, Nucl. Mater. Energy **16** (2018) 181-190. 1
[148] SCHLEIFE A., KANAI Y., CORREA A.A., Accurate atomistic first-principles calculations of electronic stopping, Phys. Rev. **B 91** (2015) 014306.
[149] OJANPERÄ A. KRASHENINNIKOV A.V., PUSKA M., Electronic stopping power from first-principles calculations with account for core electron excitations and projectile ionization, Phys. Rev. **B 89** (2014) 035120.
[150] MATIAS F. et al., Nonlinear stopping effects of slow ions in a no-free-electron system: Titanium nitride, Phys. Rev. **A 100** (2019) 030701.
[151] MORO M.V., BAUER P., PRIMETZHOFER D., Experimental electronic stopping cross section of transition metals for light ions: Systematics around the stopping maximum, Phys. Rev. **A 102** (2022) 022808.
[152] MORO M.V. et al., Experimental electronic stopping cross section of tungsten for light ions in a large energy interval, Nucl. Instr. Meth. B 498 (2021) 1-8.

List of Acronyms

Acronym	Meaning
AMS	Accelerator Mass Spectroscopy
ERDA	Elastic Recoil Detection Analysis
GDOES	Glow Discharge Optical Emission Spectroscopy
GIC	Gas Ionization Chamber (detector)
HIERDA	Heavy Ion ERDA
IBA	Ion Beam Analysis
ILW	ITER-Like Wall
JET	Joint European Torus
JET-C	JET with Carbon wall
JET-ILW	JET with ITER-Like Wall
LEIS	Low Energy Ion Source
LIAS	Laser-Induced Ablation Spectroscopy
LIBS	Laser-Induced Breakdown Spectroscopy
LID	Laser-Induced Desorption
NRA	Nuclear Reaction Analysis
PFC	Plasma-Facing Components
PFM	Plasma-Facing Materials
RBS	Rutherford Backscattering Spectrometry
RF	Radio Frequency
RGA	Residual Gas Analyser
RH	Remote Handling
SIGMA	Set-up for In-situ Growth, Material modification and Analysis
SIMS	Secondary Ion Mass Spectroscopy
TDS	Thermal Desorption Spectroscopy
ToF-ERDA	Time-of-Flight ERDA/HIERDA